LOW TEMPERATURE PROPERTIES OF SOME Er-RICH INTERMETALLIC COMPOUNDS

K.A. Gschneidner, Jr.,[1,2] A.O. Pecharsky,[1] Lucas Hale,[1] and V.K. Pecharsky[1,2]

[1]Ames Laboratory

[2]Department of Materials Science and Engineering, Iowa State University, Ames, Iowa 50011-3020, USA

ABSTRACT

The low temperature volumetric heat capacity (~3.5 to 350 K) and magnetic susceptibility (~4 to 320 K) of Er_3Rh, Er_3Ir, Er_3Pt, Er_2Al, and Er_2Sn have been measured. All of the compounds order antiferromagnetically (or ferrimagnetically), and most exhibit more than one magnetic ordering transition. The volumetric heat capacities in general are smaller than those of the prototype magnetic regenerator materials, except for Er_3Ir in the 12 to 14 K temperature range.

INTRODUCTION

Lanthanide materials have been used as low temperature (<20 K) regenerators since 1990. Capitalizing on the large magnetic entropies of the lanthanides Toshiba scientists [1,2] lowered the low temperature limit of a two stage Gifford-McMahon (G-M) cryocooler from ~10 K to ~4 K by replacing Pb in the low temperature stage with Er_3Ni. Subsequently, Nd [3] and $HoCu_2$ [4] have been utilized for cooling down to ~4 K, while Er and Er-Pr alloys (up to 50 at.% Pr) have been suggested as a replacement for Pb [5,6] as the intermediate temperature (~10 to ~60 K) range regenerator material. More recently Tanaeva *et al.* [7] proposed $GdAlO_3$, which orders at 3.8 K, as the magnetic material for the coldest section of the regenerator. Today research is still being conducted to find improved regenerator materials, which order magnetically below 20 K, in order to enhance the performance of Stirling, G-M, and pulse tube cryocoolers. Below, we summarize our recent research on five Er-rich materials: Er_3Rh, Er_3Ir, Er_3Pt, Er_2Al, and Er_2Sn.

EXPERIMENTAL DETAILS

The alloys were prepared by arc-melting stoichiometric amounts of the component materials on a water cooled copper hearth under an argon atmosphere. The alloys were

TABLE 1. Lattice Parameters, Unit Cell Volumes, and X-ray Densities of Er_3Rh, Er_3Ir, Er_3Pt, and Er_2Al.

Compound	Lattice Parameter (Å)			Unit Cell Volume ($Å^3$)	Density (g/cm^3)
	a	*b*	*c*		
Er_3Rh	7.1010(2)	9.2525(4)	6.2443(2)	410.3(1)	9.789(1)
Er_3Ir	7.1671(4)	9.0599(5)	6.3084(3)	409.6(1)	11.252(2)
Er_3Pt	7.013(1)	9.386(2)	6.369(1)	419.3(2)	11.039(6)
Er_2Al	6.4980(4)	5.0320(3)	9.2999(7)	304.1(1)	7.896(2)

turned over from 5 (Er_2Sn) to 15 times (Er_3Ir) and remelted to ensure a homogeneous ingot. Weight losses after melting were negligible. The Er was obtained from the Materials Preparation Center of the Ames Laboratory and it was 99.8+ atomic percent pure. The precious metals, Al, and Sn were obtained from commercial sources and were 99.9+ atomic percent pure. The x-ray powder diffraction data were collected on an automated Scintag powder diffractometer using Cu-K_α radiation. All of the samples were found to be single-phase materials within the limitations of the x-ray technique (typically 2 to 5 vol.% of an impurity phase) and, therefore, none of the intermetallic alloys were heat treated.

The magnetic measurements were carried out on a model 7225 Lake Shore magnetometer. The dc magnetization was measured from ~4 to ~320 K in dc fields of 1.0 to 10 kOe. The heat capacities at constant pressure were measured using an adiabatic heat-pulse-type calorimeter [8] from ~3.5 to ~350 K in zero magnetic field.

RESULTS AND DISCUSSION

X-ray Diffraction

The Er_3M (where M = Rh, Ir, and Pt) intermetallic compounds were found to crystallize in the orthorhombic Fe_3C, cementite-type structure ($D0_{11}$), space group Pnma. The Er_2Al phase was found to form the orthorhombic Co_2Si-type structure (C37), space group Pnma. The lattice parameters, unit cell volumes, and the x-ray densities are listed in TABLE 1. The crystal structure of Er_2Sn is unknown, and we made no attempt to determine it. The lattice parameters of the three Er_3M phases and Er_2Al are in good agreement with those published previously [9].

Magnetic Properties

The magnetic properties of the three Er_3M phases, Er_2Al, and Er_2Sn are given in TABLE 2. The paramagnetic effective magnetic moments, p_{eff}, for the Er-rich compounds

TABLE 2. Magnetic Properties of Er_3Rh, Er_3Ir, Er_3Pt, Er_2Al and Er_2Sn.

Compound	Curie-Weiss Behavior		Magnetic Ordering Temperatures (K)[a]		
	p_{eff} (μ_B/Er)	θp (K)	Highest	Middle	Lowest
Er_3Rh	9.59	-27.6	34.2[b]	26.7	--
Er_3Ir	9.93	-19.2	13.2	12.5	5.4
Er_3Pt	9.68	-20.8	14.4	8.5	--
Er_2Al	--	--	8.6	c	--
Er_2Sn	9.59	-20.8	38.8	<4 K	--

a --- from heat capacity measurements.
b --- see text, heat capacity of Er_3Rh.
c --- a lower magnetic transition may exist below 3.5 K.

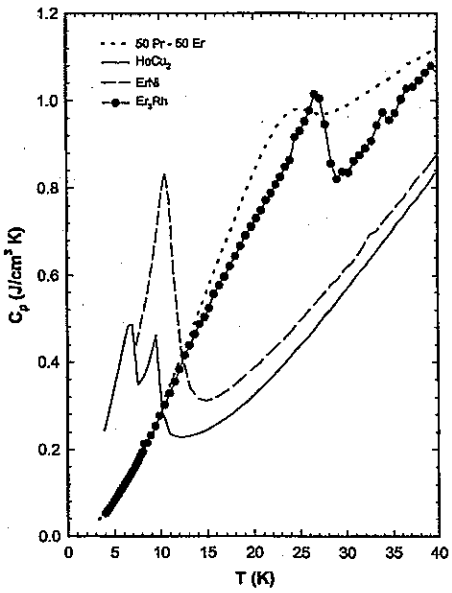

FIGURE 1. The volumetric heat capacity of Er_3Rh from ~3.5 to 40 K, along with those of $HoCu_2$, ErNi and 50 Pr-50 Er.

are slightly larger than the theoretical value of 9.58 μ_B; the largest deviation is for Er_3Ir which is 3.6% larger. The paramagnetic Curie temperature, θ_p, is negative for all of the intermetallic compounds indicating that the Er moments are aligned antiferromagnetically (or ferrimagnetically). The highest magnetic ordering temperature (TABLE 2) for each compound is in good agreement with the corresponding θ_p values. The existence of several peaks in the heat capacity vs. temperature plots (TABLE 2, and FIGS. 1-5) indicate that the magnetic ordering processes are quite complex, especially for the Er_3M phases. This is discussed in more detail in the next section on the heat capacity results.

Heat Capacity

The volumetric low temperature heat capacities of Er_3Rh, Er_3Ir, Er_3Pt, Er_2Al, and Er_2Sn as a function of temperature are shown in FIGS. 1 through 5, respectively, along with the volumetric heat capacity of several commonly used regenerator materials $HoCu_2$, ErNi, and 50 Pr-50 Er.

The heat capacity vs. temperature plot of Er_3Rh (FIG. 1) shows the existence of a typical λ-like heat capacity peak at 26.7 K, with a minor anomaly at 34.2 K, however, this could be due to experimental scatter of the data points. The shoulder on the low temperature side of the main peak (26.7 K) may be indicative of another magnetic ordering process. Additional work, such as neutron scattering, is necessary to confirm whether or not the minor anomaly at 34.2 K, and/or the shoulder at 26.7 K are due to magnetic ordering. The volumetric heat capacity of Er_3Rh, except for a two degree interval around 26 K, is less than that of the 50 Pr-50 Er solid solution alloy, and thus this Er-rich

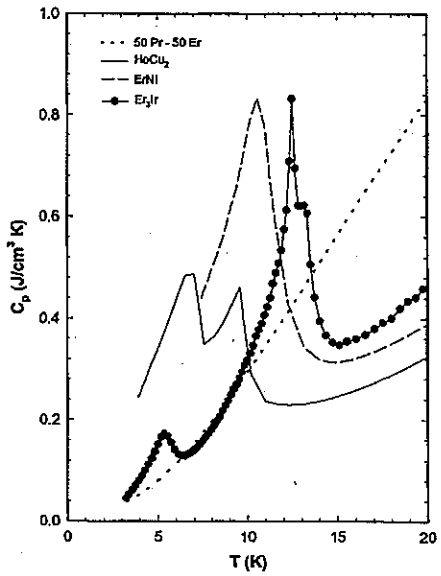

FIGURE 2. The volumetric heat capacity of Er_3Ir from ~3.5 to 20 K, along with those of $HoCu_2$, ErNi and 50 Pr-50 Er.

intermetallic compound is not likely to be utilized as a regenerator material because it is a brittle compound while the Pr-Er alloy is ductile and thus is easily fabricated into various shapes, i.e. sheet, foil, wire. Furthermore, Rh is prohibitively expensive compared to either Pr or Er.

The volumetric heat capacity of Er_3Ir as a function of temperature from ~3.5 to 20 K is presented in FIG. 2, where it is seen that two magnetic ordering arrangements occur within 1 K of each other, followed by a third one at ~5 K. The upper ordering process at 13.2 K is probably a paramagnetic to an antiferromagnetic-like alignment of spins which then undergoes a first order magnetic transition to another spin structure, probably also with an antiparallel alignment of spins. The sharp spike of the heat capacity peak at 12.5 K is indicative of a first order transition. The typical λ-like heat capacity peak at ~5 K is of second order and is probably due to spin reorientation. The double heat capacity peaks at 12-14 K make the Er_3Ir an attractive candidate for a regenerator material in which a high volumetric heat capacity is required between 12 and 14 K. However, the brittleness of this intermetallic compound and the cost of Ir will tend to limit its utilization as a cryocooler regenerator material.

The low temperature (~3.5 to 20 K) volumetric heat capacity of Er_3Pt is shown in FIG. 3. It is seen that there are at least two broad bumps at 8.5 and 14.4 K which we believe is evidence of magnetic ordering. The broad anomalies are in sharp contrast to the distinct peaks exhibited by Er_3Rh (FIG. 1) and Er_3Ir (FIG. 2). The 14.4 K bump is probably due to a paramagnetic to an antiferromagnetic (or a ferrimagnetic) transition, while the lower bump is probably due to a spin reorientation transition. The low heat capacity of Er_3Pt relative to the prototype materials indicates that Er_3Pt would not be considered as a magnetic regenerator material below 20 K.

The existence of multiple magnetic transitions in the Er_3M phases (FIGS. 1-3) is not unexpected in view of the crystal structure of these three intermetallic compounds, the orthorhombic Fe_3C, cementite ($D0_{11}$) type structure. In the $D0_{11}$ type structure the Er

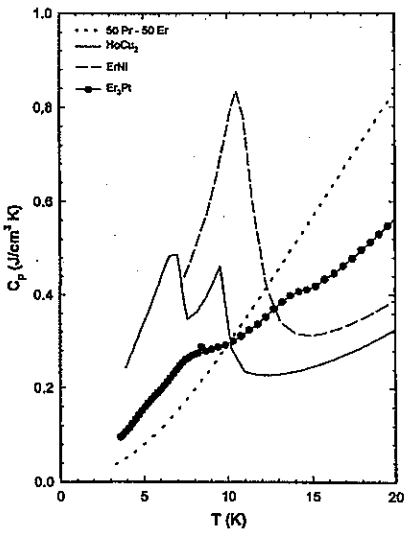

FIGURE 3. The volumetric heat capacity of Er_3Pt from ~3.5 to 20 K, along with those of $HoCu_2$, ErNi and 50 Pr-50 Er.

atoms occupy two different crystallographic sites (a 4-fold site and an 8-fold site) which increases the likelihood of an antiparallel alignment of Er spins on the two different sites.

The volumetric heat capacity of Er_2Al from ~3.5 to 20 K is shown in FIG. 4. The λ-like heat capacity peak at 8.6 K and the negative value of the paramagnetic Curie temperature (TABLE 2) indicate that Er_2Al undergoes a second order paramagnetic to antiferromagnetic (or ferrimagnetic) transition at this temperature. The upward trend of the

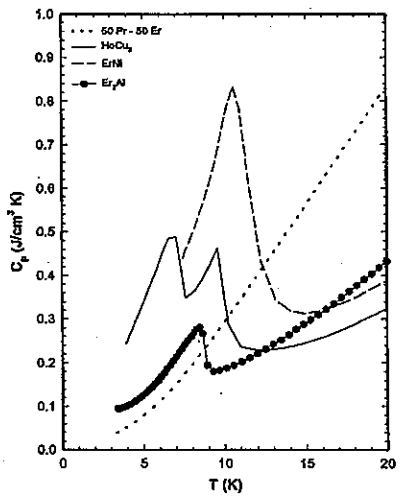

FIGURE 4. The volumetric heat capacity of Er_2Al from ~3.5 to 20 K, along with those of $HoCu_2$, ErNi and 50 Pr-50 Er.

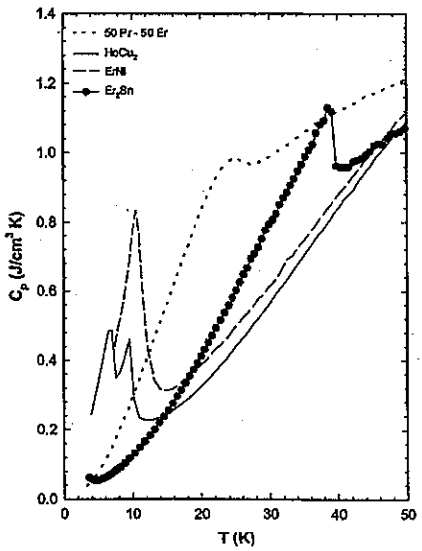

FIGURE 5. The volumetric heat capacity of Er_2Sn from ~3.5 to 50 K, along with those of $HoCu_2$, ErNi and 50 Pr-50 Er.

C_p vs. T plot below 5 K suggests that Er_2Al may undergo another magnetic transition below 3.5 K, but we have been unable to confirm this since 3.5 K is the low temperature limit of our heat capacity apparatus. The low heat capacity of Er_2Al relative to the three best cryocooler regenerator materials indicates that Er_2Al would not be a good candidate as a magnetic regenerator material below 20 K.

The volumetric heat capacity of Er_2Sn from ~3.5 to 50 K is shown in FIG. 5. Since the crystal structure of Er_2Sn is not known the density of Er_2Sn was estimated to be 8.477 g/cm^3 by assuming it was equal to 2/3^{rds} that of Er and 1/3rd that of white (metallic) Sn (i.e. 7.30 g/cm^3). The true volumetric heat capacity is probably within a few percent of that shown in FIG. 5. As is evident, there is a definite second order magnetic transition at 38.8 K, whereby the paramagnetic phase transforms to an antiferromagnetic (or a ferrimagnetic) phase. The scatter of the heat capacity values between 40 and 50 K is probably due to experimental difficulties associated with poor thermal conductivity and not magnetic ordering(s). The absence of magnetic ordering above 40 K is also confirmed by magnetic susceptibility measurements which show only one transition at ~39 K. Although the heat capacity of Er_2Sn above 18 K is significantly greater than that of $HoCu_2$ and ErNi, it is clearly inferior to that of the 50 Pr-50 Er solid solution alloy except at ~39 K where it is about the same. The upturn in heat capacity below ~5 K suggests that Er_2Sn may undergo another magnetic transition below 3.5 K, but additional measurements are needed to verify this.

SUMMARY

The crystal structures of the Er_3M (where M = Rh, Ir, and Pt) and Er_2Al have been confirmed. Magnetic measurements show that the Er_3M, Er_2Al, and Er_2Sn phases order antiferromagnetically (or ferrimagnetically) at various temperatures ranging from 8.6 K

(Er_2Al) to 38.8 K (Er_2Sn), and that most of them also exhibit an additional magnetic transition. Except for Er_3Ir, the volumetric heat capacities are small and these intermetallic compounds are, therefore, of little interest as magnetic regenerator materials for cryocooler applications. Er_3Ir exhibits two magnetic transitions in the 12 to 14 K temperature interval, and as a result the volumetric heat capacity in this region is significantly larger than those of any of the standard commercially utilized cryocooler regenerator materials.

ACKNOWLEDGEMENT

This manuscript has been authored by Iowa State University of Science and Technology under Contract No. W-7405-ENG-82 with the U.S. Department of Energy. This work was supported by the Office of Basic Energy Sciences, Materials Science Division of the U.S. DOE.

REFERENCES

1. Sahashi, M., Tokai, Y., Kuriyama, T., Nakagome, H., Li, R., Ogawa, M. and Hashimoto, T., *Adv. Cryogenic Eng.*, **35**, pp. 1175-1182 (1990).
2. Kuriyama, T., Hakamada, R., Nakagome, H., Tokai, Y., Sahashi, M., Li, R., Yoshida, O., Matsumoto, K. and Hashimoto, T., *Adv. Cryogenic Eng.*, **35**, pp. 1261-1269 (1990).
3. Ackermann, R.A., *Cryogenic Regenerative Heat Exchangers*, Plenum Press, New York, 1997, p. 98.
4. Satoh, T., Onishi, A., Umehara, I., Adachi, Y., Sato, K. and Minehara, E.J. in *Cryocoolers 11*, edited by R. G. Ross, Jr., Kluwer Academic/Plenum Publishers, New York, pp. 381-386.(2001).
5. Gschneidner, K.A., Jr., Pecharsky, A.O. and Pecharsky, V.K. in *Cryocoolers 11*, edited by R. G. Ross, Jr., Kluwer Academic/Plenum Publishers, New York, 2001, pp. 433-441.
6. Kashani, A., Helvensteijn, B.P.M., Maddocks, J.R., Kittel, P., Feller, J.R., Gschneidner, K.A., Jr., Pecharsky, V.K. and Pecharsky, A.O., *Adv. Cryogenic Eng.*, **47**, pp. 985-991 (2002).
7. Tanaeva, I.A., Ikeda, H., van Bokhoven, L.J.A., Matsubara, Y., and de Waele, A.T.A., *Cryogenics* **43**, pp. 441-448 (2003).
8. Pecharsky, V.K., Moorman, J.O., and Gschneidner, K.A., Jr., *Rev. Sci. Instrum.* **68**, pp. 4196-4207 (1997).
9. Daams, J.L.C., Villars, P., and van Vucht, J.H.N., *Atlas of Crystal Structure Types for Intermetallic Phases*, Vols. 1-4, ASM International, Materials Park, Ohio (1991).